

Assessment of Renal Cell Carcinoma Subtypes using Multidetector Computed Tomography

Diddi Vamshi Kiran

Assistant Professor, Department of Radiology, Prathima Institute of Medical Sciences and Research, Naganoor, Karimnagar, Telangana

Received: 04-06-2023 / Revised: 10-07-2023 / Accepted: 01-08-2023

Corresponding author: Dr. Diddi Vamshi Kiran

Conflict of interest: Nil

Abstract:

Background: Renal cell carcinoma (RCC) is the second most common urologic neoplasm, after prostate cancer in men and bladder cancer in women. The prevalence of RCC has been increasing in recent years. This is likely due to several factors, including changes in diet and lifestyle, as well as increased awareness of the disease. Our study aims to recognize diverse demographic attributes among RCC patients, examine varied characteristics of subtypes using multidetector computed tomography (MDCT), and ascertain the distinguishing traits among these subtypes.

Methods: This study included 25 patients who had undergone pre-operative CT scans at our institution. The scans were performed according to our renal mass protocol, which includes four phases: unenhanced, corticomedullary, nephrographic, and excretory. All patients had a confirmed pathological diagnosis of a specific subtype of renal cell carcinoma (RCC).

Results: This study identified four distinct subtypes of renal cell carcinomas (RCCs): clear cell RCC (CRCC), papillary RCC (PRCC), Xp 11.2 translocation-TFE3 carcinoma (TRCC), and chromophobe RCC (ChRCC). CRCC was the most common subtype, followed by PRCC. The majority of tumors were small (≤ 200 cc) and had smooth margins. They showed varied enhancement patterns and signs of cystic degeneration. A small portion of the tumors displayed calcifications. The tumor enhancement ratio was above 0.3. The density of solid tumor areas in CECT scans was high and closely resembled the attenuation values of the renal cortex. In contrast, papillary, chromophobe, and TRCC types had relatively lower attenuation.

Conclusion: This study found that tumor attenuation is the most important differentiating feature between different subtypes of renal cell carcinoma (RCC). However, other parameters assessed by multi-detector computed tomography (MDCT) such as size at presentation, heterogeneity, tumor spread, and tumor/aorta enhancement ratio can also help to distinguish between different subtypes of RCC.

Keywords: Renal Cell Carcinoma (RCC), Multi-Detector Computed Tomography (MDCT), Papillary Renal cell carcinoma (PRCC).

This is an Open Access article that uses a funding model which does not charge readers or their institutions for access and distributed under the terms of the Creative Commons Attribution License (<http://creativecommons.org/licenses/by/4.0>) and the Budapest Open Access Initiative (<http://www.budapestopenaccessinitiative.org/read>), which permit unrestricted use, distribution, and reproduction in any medium, provided original work is properly credited.

Introduction

Renal cell carcinoma (RCC) ranked as the 17th most prevalent cancer type, constituting 2.0% of all global cancer diagnoses in the year 2018 [1]. The incidence of secondary primary cancers has increased due to advancements in diagnostic imaging technologies and the treatment of common cancers. [2] Warren and Gates established the diagnostic criteria for multiple primary malignancies, which remain valid today [3]. The occurrence of a single patient having multiple primary cancers ranges from 0.7% to 11% of all carcinoma cases. [4] Patients with renal cell carcinoma are susceptible to developing synchronous primary cancers, as evidenced by a few reported cases of concurrent occurrence of renal cell carcinoma with other malignancies [5–7].

"In 2013, the International Society of Urological Pathology put forth a revised classification for RCC, which retained the WHO proposal while suggesting the incorporation of five newly characterized types of renal neoplasms. Additionally, three other types, viewed as emerging entities, were recommended for inclusion. [7]

Imaging techniques play a pivotal role in RCC diagnosis, leading to a trend of identifying tumors in their earlier stages. Moreover, these methods are crucial for both staging and treatment planning.8 Many renal tumors are incidentally detected during imaging scans conducted for urological or other medical concerns. Previous studies have even demonstrated the potential for histological diagnosis

of renal tumors based on their imaging characteristics. Among these techniques, computed tomography (CT) has gained widespread use for RCC evaluation due to its ability to provide comprehensive insights into the tumor itself, perinephric extension, involvement of the renal vein, and lymphatic spread. [8, 9] Helical CT, in particular, permits the analysis of tumor enhancement patterns. Prior research consistently emphasized that a more intense enhancement pattern stood out as the key distinguishing feature among various RCC subtypes.

Furthermore, a study conducted by Herts et al. [10] introduced an additional parameter known as the tumor-to-aorta enhancement ratio. This parameter significantly enhances the sensitivity of diagnosing papillary cell carcinoma, increasing its diagnostic accuracy by 50%. With this background the objective of this study was to investigate the demographic attributes and key imaging observations of histological variants of RCC within the author's present geographical setting, utilizing multidetector CT (MDCT). Additionally, the study aimed to explore critical imaging traits that facilitate differentiation among these subtypes.

Material and Methods

This retrospective study was conducted in the Department of Radiology, Department of Radiology, Prathima Institute of Medical Sciences, Nagunoor, Karimnagar, Telangana State. Institutional Ethical approval was obtained for the study.

This study was approved by the Institutional Review Board and used medical records and images from 25 patients who had undergone pre-operative CT scans at our institution. The scans were performed according to our renal mass protocol, which includes four phases: unenhanced, corticomedullary, nephrographic, and excretory. All patients had a confirmed pathological diagnosis of a specific subtype of renal cell carcinoma (RCC).

CT Examination

A multi-detector computed tomography (MDCT) examination was performed on each patient using a 16-slice GE Lightspeed CT scanner. This type of scanner uses multiple detectors to acquire images more quickly and with better resolution than traditional CT scanners. The scans were performed during suspended inspiration, which means that the patient held their breath during the scan to minimize motion artifacts. Intravenous contrast was administered as Omnipaque 300 (Iohexol) 150 mL bolus containing 40-45 g of iodine through the antecubital vein at a rate of 2-4 mL/s. This contrast agent helps to highlight the blood vessels and structures in the body, making them easier to see in the images.

The scanning parameters were as follows:

- Collimation: 1.3 mm
- Pitch: 2:1
- Scan time: subsecond
- kVp: 120
- mAs: 210

Images were obtained in four phases: unenhanced, corticomedullary, nephrographic, and excretory. The unenhanced scan was performed without any contrast agent, while the other three scans were performed after the contrast agent had been injected.

Imaging Evaluation

Two radiologists independently reviewed the contrast-enhanced computed tomography (CECT) images in consensus. The following parameters were studied:

- Demographic features of the patients
- Imaging features of the renal tumors on plain and CECT in four phases, including lesion size, presence, type and attenuation, calcification, characteristics of tumor spread, and metastases
- Attenuation values were obtained in all four phases using a region of interest (ROI) of 1-3 cm². The average of three readings was taken along the circumference of the tumor. Attenuation values were obtained separately for the cortex and solid-enhancing area of the tumor.

The demographic features of the patients included their age, sex, race, and medical history. The imaging features of the renal tumors included their size, shape, location, attenuation, and presence of calcification. The characteristics of tumor spread included the presence of lymph node metastases and distant metastases. The attenuation values were used to assess the density of the tumor and to help determine the type of tumor. The purpose of this study was to evaluate the use of MDCT in the diagnosis and characterization of renal tumors. The results of the study showed that MDCT is a valuable tool for the diagnosis and characterization of renal tumors. It can accurately depict the size, shape, location, and attenuation of tumors, as well as the presence of calcification and tumor spread.

Results

A total of 25 cases were recorded in the study the age range was 38 years to 70 years. the incidence of RCC was highest in patients in the 40-59 age group. The details are depicted in Figure 1. The mean age of the cohort was 58.58 ± 8.5 years. Out of the 25 cases, 12 cases were males and 13 cases were females and the side of the kidney involved showed 13 cases with left kidney involvement and 12 cases with right kidney involvement and no difference in the cases.

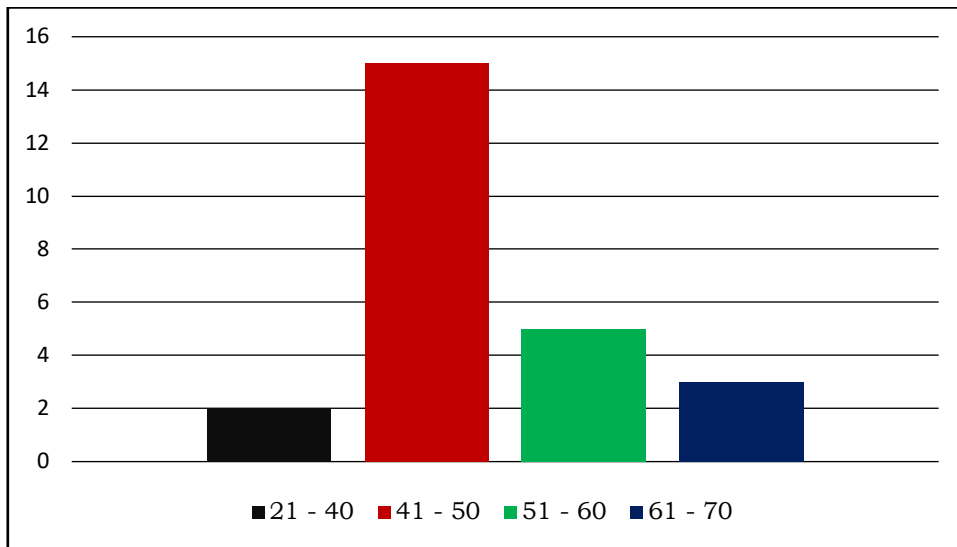


Figure 1: Age-wise distribution of cases included in the study

In our study, we identified four distinct subtypes of renal cell carcinomas (RCCs). These subtypes included clear cell RCC (CRCC), papillary RCC (PRCC) as shown in Figure 2, Xp 11.2 translocation-TFE3 carcinoma (also known as translocation RCC or TRCC), and chromophobe RCC (ChRCC). Among these subtypes, the most prevalent was clear cell carcinoma, followed by papillary RCC. We observed one instance of translocation RCC and one case of chromophobe RCC, as demonstrated in Figure 2.

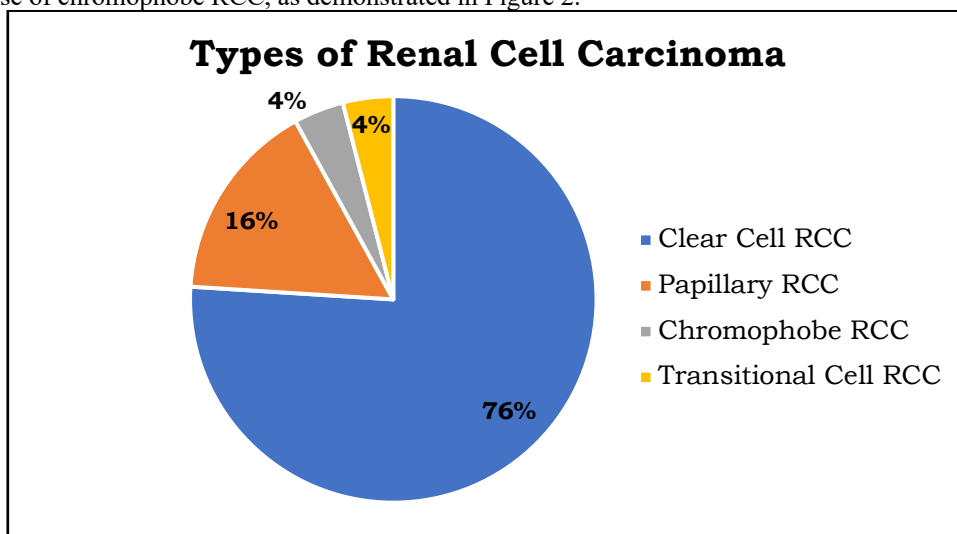


Figure 2: Types of Renal Cell carcinoma detected in the cases of the study

Table 1: Distribution profile of different renal cell carcinoma in the cases of the study

	Clear cell CRCC (n=19)	PRCC (n=4)	Chromophobe ChRCC (n=1)	Translocation TRCC (n=1)
Age group				
21 – 40	0 (0.00)	0 (0.00)	0 (0.00)	1 (100.0%)
41 – 50	11 (57.89%)	3 (75.0)	1 (100.0%)	0 (0.00)
51 – 60	5(26.32%)	1 (25.0%)	0 (0.00)	0 (0.00)
61 - 70	3 (15.79%)	0 (0.00)	0 (0.00)	0 (0.00)
Sex				
Male	9 (47.37%)	3 (75.0%)	0 (0.00)	0 (0.00)
Female	10 (57.89%)	1 (25.0%)	1 (100.0%)	1 (100.0%)

The majority of tumors (57.89%) initially had a smaller size (≤ 200 cc) and smooth margins (89%). These tumors showed a varied enhancement pattern

and indications of cystic degeneration (89%). A smaller portion (10%) of these tumors displayed calcifications. The ratio of tumor enhancement to

that of the aorta was above 0.3. The density of solid tumor areas in contrast-enhanced CT (CECT) scans was remarkably high and closely resembled the attenuation values of the renal cortex (75-145 HU).

In contrast, papillary, chromophobe, and translocation RCC types had relatively lower attenuation, as shown in Table 2.

Table 2: Distribution of cases with RCC according to the tumor characteristics

	Clear cell CRCC (n=19)	PRCC (n=4)	Chromophobe ChRCC (n=1)	Translocation TRCC (n=1)
Size (%)				
≤ 200 cc	11(57.89%)	4(100%)	0	1(100%)
≥ 200 cc	8(42.11%)	0	1(100%)	0
Margins (%)				
Smooth	17(89.47%)	3(75.0%)	1(100%)	1(100%)
Irregular	2(10.53%)	1(25.0%)	0	0
Calcifications				
Present	2(10.53%)	4(100%)	1(100%)	0
Absent	17(89.47%)	0	0	1(100%)
Cystic Degeneration				
Present	17(89.47%)	2(50.0%)	0	0
Absent	2(10.53%)	2(50.0%)	1(100%)	1(100%)

Table 3: Distribution of cases with RCC according to the tumor CECT characteristics

	Clear cell CRCC (n=19)	PRCC (n=4)	Chromophobe ChRCC (n=1)	Translocation TRCC (n=1)
Enhancement Pattern (%)				
Homogeneous	11	3	1	1
Heterogeneous	08	1	0	0
Tumor to aorta enhancement ratio				
< 0.3	00	3	1	0
0.3	00	1	0	1
>0.3	19	0	0	0
CECT attenuation of solid areas				
Corticomedullary phase	76 – 145 HU	40 – 66 HU	90HU	94 HU

Papillary Renal Cell Carcinoma

The age distribution for PRCC resembled that of clear cell carcinoma, occurring around the ages of 45 to 49 years. The male-to-female ratio was 3:1. Our investigation revealed a higher tendency for PRCC to affect the left kidney.

The initial lesion size was smaller than that of ChRCC (ranging from 30 to 90 cubic centimeters, and no instances of calcifications within the lesion were detected. Maximum attenuation on non-contrast-enhanced computed tomography (NECT) was recorded as 43 Hounsfield units (HU), while contrast-enhanced CT (CECT) revealed an attenuation of 60 HU during the corticomedullary phase, with the majority demonstrating a consistent and uniform enhancement pattern.

The ratio of tumor enhancement to aorta enhancement was found to be less than 0.3, ranging between 0.15 and 0.23. Among the observed lesions, all exhibited perinephric spread, while no instances of spread to neighboring organs, the renal vein, or the ureter were observed. In terms of lymphatic spread, 50% of cases showed regional lymph node involvement, while distal lymph node spread was

absent. In the context of our study, cases of pRCC did not display any distal organ metastases.

Translocation Renal Cell Carcinoma

Within our study, a solitary case of translocation RCC was identified in a pediatric female patient, affecting the left kidney, as outlined in Table 1. The tumor's initial size upon presentation was measured at 40 cubic centimeters, featuring smooth margins and devoid of calcifications and degeneration, as specified in Table 2.

The tumor's characteristics included a uniform enhancement pattern. Notably, the attenuation of the mass was higher compared to pRCC in both NECT and CECT, yet lower in contrast to cRCC. The tumor-to-aorta enhancement ratio was calculated as 0.3. This subtype exhibited regional lymph node spread, while other modes of dissemination were not identified.

Chromophobe Renal Cell Carcinoma

One instance, involving a 29-year-old female, was presented within our study. The lesion's size upon presentation exceeded 200 cubic centimeters. The lesion exhibited a uniform density akin to the renal

parenchyma, displaying lobulated margins along with internal calcifications. No evidence of degeneration was observed. Post-contrast HU measurements of the lesion remained below 100, indicating a histologically hypovascular nature. Notably, the tumor demonstrated its maximal

enhancement during the nephrographic phase, surpassing other subtypes in this regard. The tumor-to-aorta enhancement ratio was measured between >0.23 and <0.3 . No distinct patterns of tumor spread were identified.

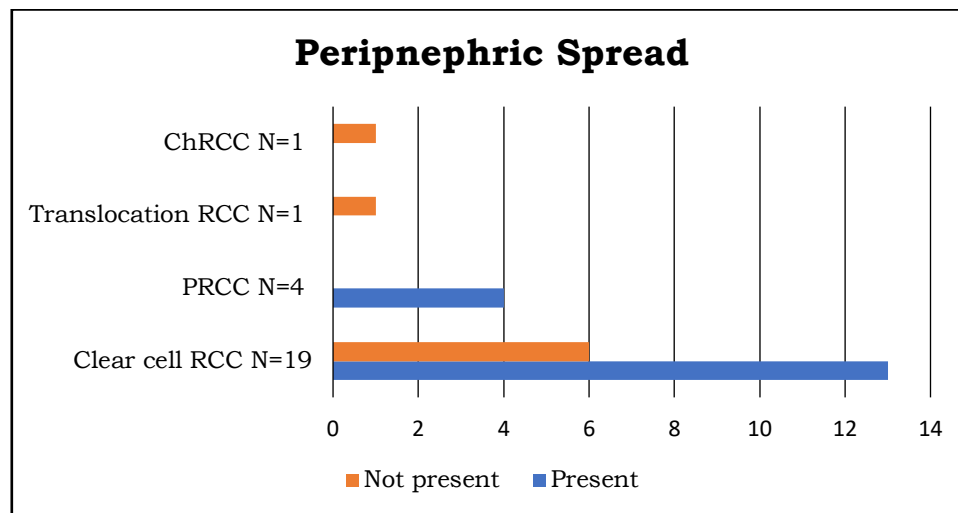


Figure 3: Perinephric Spread pattern of different RCC

Disease Dissemination Patterns

The primary mode of spread of the cRCC disease involved the perinephric fat predominantly 13/19(68.42%). There was a lower occurrence of local spread to neighboring organs in 3/19(15.79%). Other observed pathways of dissemination included passage through the ureter 3/19(15.79%), renal vein 6/19(31.57%), and the inferior vena cava (IVC) 4/19(21.05%). The mode of lymphatic spread to regional lymph nodes exhibited a higher prevalence 15/19(78.94%). No instances of distal lymph node involvement were identified in our research. Metastatic spreading was less frequent (10.52%), with the majority (60%) targeting the lungs, followed by the liver and bones (specifically the lumbar vertebrae).

Discussion

The categorization of renal cell carcinoma (RCC) primarily relied on the microscopic characteristics of the tumor as well as its genetic anomalies. Each distinct subtype is linked to varying prognoses and behaviors of the tumor. [11] Patients who are diagnosed with papillary carcinoma and the chromophobe subtype tend to exhibit a higher 5-year survival rate compared to those with the conventional RCC subtype. [11, 12] Numerous research studies have been conducted to discern the computed tomography (CT) features unique to the different subtypes of RCC. These investigations have revealed that conventional RCC often demonstrates robust enhancement similar to the renal cortex. In our study, we observed differing

enhancement patterns among the four RCC subtypes, notably observing high-attenuation values in the corticomedullary phase for clear cell carcinoma (cRCC). This subtype exhibited a vigorous enhancement pattern across all phases, as indicated by high-attenuation values, surpassing the patterns seen in other tumor types. These findings align with parallel studies, which also reported similar enhancement patterns. [13, 14]

The robust enhancement pattern exhibited by clear cell renal cell carcinoma (CRCC) can be attributed to its well-developed vascular network and alveolar architecture, as evidenced by histological examination. [11, 13] In conjunction with this enhancement pattern, the presence of calcifications and cystic degeneration serves as noteworthy distinguishing characteristics. The combination of these features aids in the differentiation of CRCC from other subtypes. The heterogeneous enhancement pattern within the tumor arises from hemorrhage and necrosis, which are apparent upon pathological examination. [11, 15] Another significant observation is the tumor-to-aorta enhancement ratio, which exceeded 0.3 in cases of CRCC. Furthermore, our study highlighted the presence of lesion spread as an additional important feature in CRCC. This spread includes an extension into the perinephric space, regional lymph nodes, and adjacent organs, as well as infiltration into the renal vein, inferior vena cava (IVC), ureter, and distant organ metastases.

Papillary carcinoma was the second most common type of cancer found in our study, with an incidence of 17%. [15] This type of cancer is characterized by a homogeneous enhancement pattern with fewer attenuation values than clear cell renal cell carcinoma (cRCC). [16, 17] This is due to the hypovascularity of the tumor. Calcifications were not found in our study, which is in contrast to other studies. This could be due to the small sample size of our study. The tumor aorta enhancement ratio was also low (<0.3), which is again consistent with the hypovascularity of the lesion. [18] In summary, papillary carcinoma is a less vascular type of cancer than cRCC. This is reflected in the homogeneous enhancement pattern and low tumor aorta enhancement ratio seen in papillary carcinoma. Calcifications are also less common in papillary carcinoma than in CRCC.

Papillary carcinoma is the second most common type of cancer found in our study. It is characterized by a homogeneous enhancement pattern with fewer attenuation values than clear cell renal cell carcinoma (cRCC). This is due to the hypovascularity of the tumor, which means that it has fewer blood vessels. Calcifications were not found in our study, which is in contrast to other studies. This could be due to the small sample size of our study. The tumor aorta enhancement ratio was also low (<0.3), which is again consistent with the hypovascularity of the lesion. In summary, papillary carcinoma is a less vascular type of cancer than cRCC. This is reflected in the homogeneous enhancement pattern and low tumor aorta enhancement ratio seen in papillary carcinoma. Calcifications are also less common in papillary carcinoma than in CRCC.

Conclusion

This study found that tumor attenuation is the most important differentiating feature between different subtypes of renal cell carcinoma (RCC). However, other parameters assessed by multi-detector computed tomography (MDCT) such as size at presentation, heterogeneity, tumor spread, and tumor/aorta enhancement ratio can also help to distinguish between different subtypes of RCC, especially clear cell renal cell carcinoma (cRCC) and other RCC subtypes. The authors of the study suggest that their findings should be confirmed and validated by larger and prospective studies. They also note that the use of MDCT to distinguish between different subtypes of RCC could help to improve patient care by guiding treatment decisions.

References

1. Bray F, Ferlay J, Soerjomataram I, Siegel RL, Torre LA, Jemal A. Global cancer statistics 2018: GLOBOCAN estimates of incidence and mortality worldwide for 36 cancers in 185

- countries. *CA Cancer J Clin.* 2018;68(6):394–424.
2. Kovacs G, Akhtar M, Beckwith BJ, Bugert P, Cooper CS, Delahunt B, Eble JN, Fleming S, Ljungberg B, Medeiros LJ, Moch H, Reuter VE, Ritz E, Roos G, Schmidt D, Srigley JR, Störkel S, van den Berg E, Zbar B. The Heidelberg classification of renal cell tumors. *J Pathol.* 1997 Oct;183(2):131-3.
3. Warren S, Gates O. Multiple primary malignant tumors. *Am J Cancer* 1932; 16:1358–1414.
4. Decastro GJ, McKiernan JM. Epidemiology, clinical staging, and presentation of renal cell carcinoma. *Urol Clin North Am.* 2008 Nov; 35(4):581-92; 6.
5. Rabbani F., Grimaldi G., Russo P. Multiple primary malignancies in renal cell carcinoma. *Journal of Urology.* 1998;160(4):1255–1259.
6. Dafashy TJ, Ghaffary CK, Keyes KT, Sonstein J. Synchronous Renal Cell Carcinoma and Gastrointestinal Malignancies. *Case Rep Urol.* 2016; 2016:7329463.
7. Delahunt B, Srigley JR, Montironi R, Egevad L. Advances in renal neoplasia: Recommendations from the 2012 International Society of Urological Pathology Consensus Conference. *Urology* 2014; 83:969-74.
8. Velez-Torres J., Guido L.P., Jorda M. Adult Renal Neoplasms: Cytology, Immunohistochemistry, and Cytogenetic Characteristics. *Surg. Pathol. Clin.* 2018;11:611–631.
9. Tataru OS, Marchioni M, Crocetto F, Barone B, Lucarelli G, Del Giudice F, Busetto GM, Veccia A, et al. Molecular Imaging Diagnosis of Renal Cancer Using ^{99m}Tc-Sestamibi SPECT/CT and Girentuximab PET-CT-Current Evidence and Future Development of Novel Techniques. *Diagnosics (Basel).* 2023 Feb 6;13(4):593.
10. Herts BR, Coll DM, Novick AC, Obuchowski N, Linnell G, Wirth SL, Baker ME. Enhancement characteristics of papillary renal neoplasms revealed on triphasic helical CT of the kidneys. *AJR Am J Roentgenol.* 2002 Feb;178(2):367-72.
11. Reuter VE, Presti JC Jr. Contemporary approach to the classification of renal epithelial tumors. *Semin Oncol* 2000; 27:124-37.
12. Bonsib SM. Risk and prognosis in renal neoplasms. A pathologist's perspective. *Urol Clin North Am* 1999; 26:643-60, viii.
13. Fujimoto H, Wakao F, Moriyama N, Tobisu K, Sakamoto M, Kakizoe T. Alveolar architecture of clear cell renal carcinomas (< or = 5.0 cm) show high attenuation on dynamic CT scanning. *Jpn J Clin Oncol* 1999; 29:198-203.
14. Wildberger JE, Adam G, Boeckmann W, Münchau A, Brauers A, Günther RW, et al. Computed tomography characterization of renal

- celltumors in correlation with histopathology. Invest Radiol 1997;32:596-601.
15. Störkel S, van den Berg E. Morphological classification of renal cancer. World J Urol. 1995;13(3):153-58.
 16. Kim JK, Kim TK, Ahn HJ, Kim CS, Kim KR, Cho KS. Differentiation of subtypes of renal cell carcinoma on helical CT scans. AJR Am J Roentgenol 2002; 178:1499-506.
 17. Choyke PL, Glenn GM, Walther MM, Zbar B, Linehan WM. Hereditary renal cancers. Radiology 2003; 226:33-46.
 18. Prasad SR, Humphrey PA, Menias CO, Middleton WD, Siegel MJ, Bae KT, et al. Neoplasms of the renal medulla: Radiologic-pathologic correlation. Radiographics 2005; 25:369-80.